atmosphere

MDPI

Article

Assessing Douro Vineyards Exposure to Tropospheric Ozone

Ana Ascenso [1,*], Carla Gama [1], Daniel Blanco-Ward [1], Alexandra Monteiro [1], Carlos Silveira [1], Carolina Viceto [2], Vera Rodrigues [1], Alfredo Rocha [2], Carlos Borrego [1], Myriam Lopes [1] and Ana Isabel Miranda [1]

[1] CESAM—Centre for Environmental and Marine Studies, Department of Environment and Planning, University of Aveiro, 3810-193 Aveiro, Portugal; carlagama@ua.pt (C.G.); dblancoward@ua.pt (D.B.-W.); alexandra.monteiro@ua.pt (A.M.); carlos.silveira@ua.pt (C.S.); vera.rodrigues@ua.pt (V.R.); cborrego@ua.pt (C.B.); myr@ua.pt (M.L.); miranda@ua.pt (A.I.M.)

[2] CESAM—Centre for Environmental and Marine Studies, Department of Physics, University of Aveiro, 3810-193 Aveiro, Portugal; carolinaviceto@ua.pt (C.V.); alfredo.rocha@ua.pt (A.R.)

* Correspondence: ascenso.a@ua.pt

Abstract: Tropospheric ozone (O_3) can strongly damage vegetation. Grapevines (*Vitis vinifera L.*), in particular, have intermediate sensitivity to ozone. Wine production is an important economic activity, as well as a pillar to the cultural identity of several countries in the world. This study aims to evaluate the risk of Douro vineyards exposure to ozone, by estimating its concentration and deposition in the Demarcated Region of Douro in Portugal. Based on an assessment of the climatology of the area, the years 2003 to 2005 were selected among the hottest years of the recent past, and the chemical transport model CHIMERE was used to estimate the three-dimensional field of ozone and its dry deposition over the Douro region with 1 km^2 of horizontal resolution. Model results were validated by comparison with measured data from the European air quality database (AirBase). The exposure indicator AOT40 (accumulated concentration of ozone above 40 ppb) was calculated and an exposure–response function was applied to determine the grapevine risk to ozone exposure. The target value for the protection of vegetation established by the Air Quality Framework Directive was exceeded on most of the Douro region, especially over the Baixo Corgo and Cima Corgo sub-regions. The results of the exposure–response functions suggest that the productivity loss can reach 27% and that the sugar content of the grapes could be reduced by 32%, but these values are affected by the inherent uncertainty of the used methodology.

Keywords: tropospheric ozone; grapevine (*Vitis vinifera* L.); air quality modelling; AOT40; dry deposition

Citation: Ascenso, A.; Gama, C.; Blanco-Ward, D.; Monteiro, A.; Silveira, C.; Viceto, C.; Rodrigues, V.; Rocha, A.; Borrego, C.; Lopes, M.; et al. Assessing Douro Vineyards Exposure to Tropospheric Ozone. *Atmosphere* **2021**, *12*, 200. https://doi.org/10.3390/atmos12020200

Academic Editors: Alfredo Rocha and Ana Isabel Miranda

Received: 18 December 2020

Accepted: 26 January 2021

Published: 2 February 2021

1. Introduction

The tropospheric ozone capability to damage vegetation has been identified and studied by many authors [1–3]. The physiological effects of ozone absorption are manifested by reducing photosynthesis, increasing ageing at the cellular level, enhancing susceptibility to diseases, decreasing growth and the reproductive capacity of plants [4,5]. High levels of ozone can therefore lead to loss of productivity and quality of agricultural fields, and consequently to economic losses.

Heck et al. [6] estimated, for instance, that 90% of the productivity loss due to air pollution in the United States results from exposure to O_3. Holland et al. [7] conducted a study in 47 European countries and concluded that ozone is responsible for economic losses of 6.7 billion euros. In the forests of Sweden, Karlsson et al. [8] estimated a loss of approximately 40 million euros per year. Mills and Harmens [9] showed that ozone effects resulted in losses of 27 million tonnes of wheat grains in 2000. Avnery et al. [10] determined that ozone could be responsible for a 10% reduction in cereal production in the European Union by 2030. Currently, tropospheric ozone is considered the most damaging atmospheric pollutant to vegetation and its impacts cannot be ignored [1,4,11].

To cause damage, the ozone first needs to be absorbed by the stomata in the plant leaf. Thus, the O_3 uptake is considerably controlled by the stomatal flux, varying as a function of the stoma opening and the O_3 ambient concentration [12,13]. The stoma role is to control the water loss and mediate gas exchanges, so, the stoma opening is reduced on hot, dry or windy days. It also opens in response to light, and close in response to decreased humidity and increased concentrations of carbon dioxide [14]. According to Emberson et al. [15], the most important factors regulating ozone uptake by plants are ambient air temperature and vapour pressure deficit, soil moisture deficit and phenology. Therefore, when studying the effects of O_3 on vegetation, it is necessary to consider not only the concentrations of ozone, which determines the exposure of the crops, but also the deposition of ozone on vegetation, which points toward the ozone uptake via the stomata [16]. Nevertheless, plants can protect themselves after the ozone is absorbed, through a process called ozone detoxification. Detoxification occurs when the plant produces antioxidants that react with O_3, thus protecting the cellular tissue. Species with high detoxification potential show a lower relationship between stomatal O_3 absorption and related phytotoxical damage [17,18]. To predict adequately the ozone impacts on vegetation, it is necessary to examine both O_3 uptake and detoxification of plants [19].

In summary, many studies are assessing the ozone damage on crops, but research is still needed to achieve a better understanding of the plant response to be able to develop numerical models that can successfully represent these processes. Moreover, available studies mainly focus on staple crops like wheat and potatoes and there are few papers regarding other types of crops like grapevines (e.g., the recent review by Blanco-Ward et al. [11]). The present work applies a numerical modelling system to assess annual ozone deposition levels on vineyards from an important Portuguese wine region, the Douro Demarcated Region (DDR), which is located in northeast Portugal. Wine production is a major economic activity in Portugal and the DDR stands out by its famous Port's Wine production.

The hot summers of the Douro region are associated with high levels of ozone in the ambient air [20]. Given the potential negative impacts of grapevine exposure to ozone and the economic interest of the region, it is important to know the temporal and spatial distribution of this pollutant in the DDR. Therefore, this study aims to assess the Douro vineyards' exposure to tropospheric ozone in recent past climate conditions representative of hot summers, by estimating O_3 concentrations and dry deposition levels and relating them with the effects on sugar content and productivity of the grapevine.

Ozone concentration and dry deposition were estimated using the air quality modelling system WRF-CHIMERE. The simulations were performed for the years 2003 to 2005 since they were some of the hottest years of the recent past. Model results were validated for the simulation period comparing them with the values measured by monitoring stations from the Portuguese and Spanish air quality monitoring networks. Then, model results were analyzed as AOT40, an accumulated ozone exposure indicator applied by the European Union (EU) to monitor and prevent vegetation damage from ozone exposure. Finally, these modelling results were related to to exposure–response functions as derived by Soja et al. [21] to estimate the potential loss of productivity and grape sugar content associated to ambient O_3 in the DDR.

The following work is organized in 4 sections: Section 2 describes the study area, the Douro Demarcated Region; methodology and model validation are presented in Section 3; results and discussion are provided in Section 4. Summary and conclusions are drawn in Section 5.

2. Description of the Study Area

The Douro Demarcated Region is the oldest controlled winemaking region in the world and is of great economic value for Portugal. It was created in 1756 and classified as a World Heritage Site for its "cultural, evolutionary and living landscape" in 2001 by the United Nations Educational, Scientific and Cultural Organization. Located within the Douro River basin in the northeastern part of Portugal, the region is known for its deep

valleys and mountainous terrain; its altitude can differ between 40 m and 1400 m [22]. The DDR is divided into three sub-regions: Baixo Corgo, Cima Corgo and Douro Superior. The topography of the region and the location of the sub-regions are shown in Figure 1.

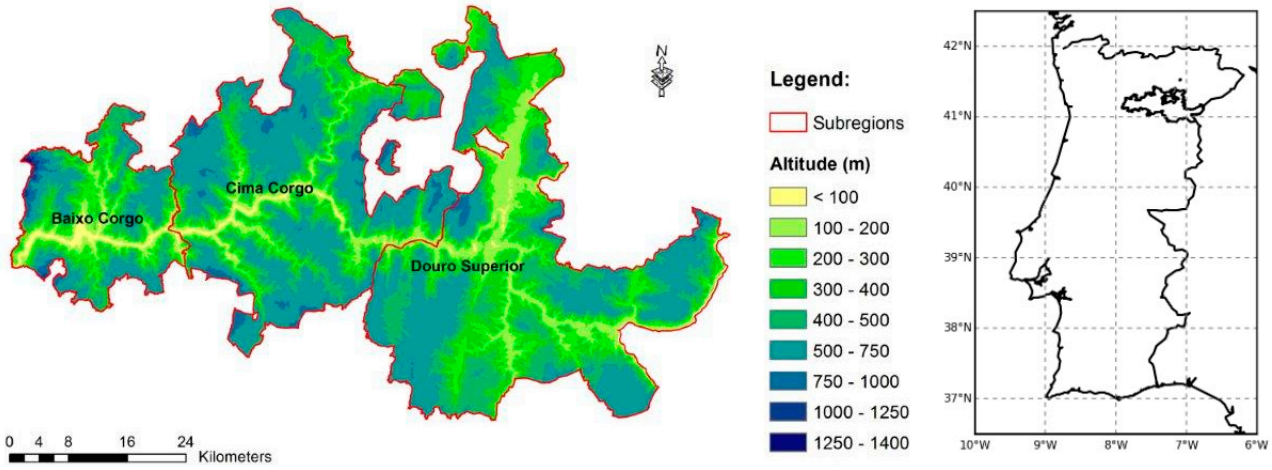

Figure 1. Case-study location, its sub-regions and topography.

The geographic characteristics of the region provide a favorable climate for wine production (temperatures between 12 and 22 °C), with an average temperature throughout the grapevine vegetative cycle of 17.8 °C. The precipitation, distributed asymmetrically, decreases in the Baixo Corgo–Douro Superior direction and presents an annual median of 950 mm [22,23]. Extreme weather has a major influence in vineyard regions. Events such as warm and cold temperature extremes, drought, extreme rain, hail, frost or thunderstorms have significant impacts in the productivity and quality of wine [24,25]. For the period 1986–2005, the Baixo Corgo region had less extreme maximum and minimum temperatures, resulting for example in less frost days (Tmin < 0 °C) or summer days (Tmax > 25 °C), when compared to Douro Superior [26].

Covering approximately 28% of all the land, vineyards are the main land-use type in the region followed by open forests and shrubs. The sub-regions with higher vineyard acreage are the Baixo and Cima Corgo, while olive groves and orchards prevail in Douro Superior [27] (Figure 2).

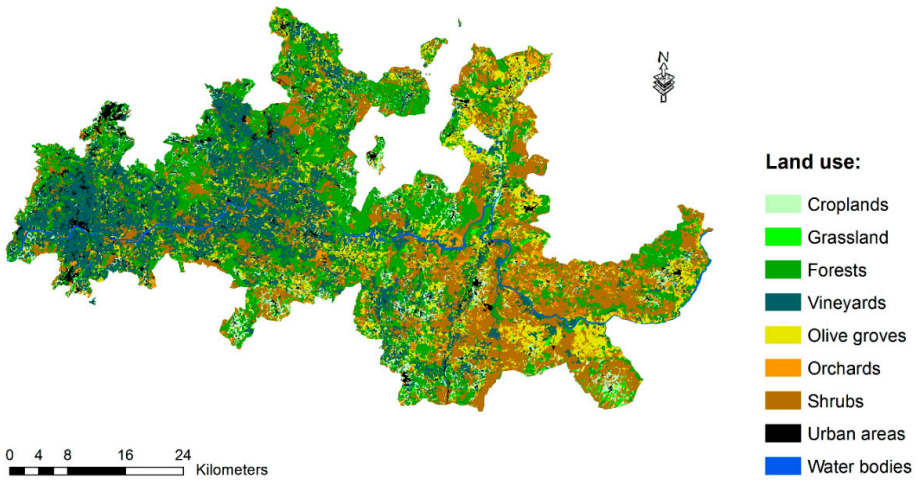

Figure 2. Douro Demarcated Region land use (source: CORINE Land Cover).

Within the DDR there are no air quality monitoring stations. The closest one is the rural background station Douro Norte, that is located 9 km northwest of the region, at an altitude of 1086 m. High ozone concentrations are generally observed at this air

quality station [28,29], thus modelling the ozone levels in the DDR will also contribute for understanding if this rural air quality station is representative of the region.

3. Methodology

To assess the grapevine exposure to tropospheric ozone, an air quality modelling system was applied for the current climate and was then validated using observational data available and compiled for the study period. The effect of ozone on vineyards was evaluated using appropriate metrics for this assessment.

3.1. WRF-CHIMERE Modelling System

The modelling system is based on the chemistry-transport model CHIMERE v2016a1 [30,31], forced by the Weather Research and Forecasting (WRF) model v3.5.1 [32].

The WRF model is a mesoscale numerical weather prediction (NWP) and atmospheric simulation system developed for both research and operational applications. A detailed description of the model can be found in the model manual [32]. The initial and boundary conditions for the simulations were driven by ERA-Interim reanalysis data (WRF-ERA), obtained from the European Centre for Medium-Range Weather Forecasts, with a horizontal resolution of approximately 79 km [33]. The boundary conditions were provided to WRF at 6-h intervals. The land use database comes from the "US Geological Survey" (USGS). The WRF model was applied using a configuration similar to the one described by Marta-Almeida et al. [34].

CHIMERE is an open access multi-scale Eulerian Chemical Transport Model (CTM), developed for simulating gas-phase chemistry [35] and aerosol formation, transport and deposition [36,37] from regional to urban scales. The initial and boundary conditions for the first domain were obtained from the LMDz-INCA (gas species and non-dust aerosols) [38] and GOCART (dust) [39] global chemical-transport models. The anthropogenic emissions were based on the EMEP inventory [40], after being processed to achieve hourly spatially resolved emissions, as required by the model. The biogenic emissions were provided by the MEGAN model [41]. In addition, the USGS land use database was also used. The chemical mechanism was MELCHIOR-2, which simulates the concentration of 44 gaseous species from a set of 120 chemical reactions; this mechanism is derived from MELCHIOR [42] following the concept of "chemical operators" [43]. CHIMERE was applied with eight vertical levels; the first layer pressure is 997 mbar and the last extends to 500 mbar. Table 1 presents a summary of the approach applied for each main process and input data considered by the air quality model.

Table 1. Summary of main CHIMERE model options and methodology used.

Process	Approach
Meteorology	Model WRF
Land use	USGS database
Anthropogenic emissions	EMEP inventory
Biogenic emissions	MEGAN model
Chemical Mechanism	MELCHIOR-2
Dry deposition	Wesely Parametrization

The CHIMERE model was set up in one-way hourly nesting configuration with four nested domains with an increasing horizontal resolution, namely 81, 27, 9 and 1 km (Figure 3). The current model setup was selected after a careful analysis where different domains were tested based on the quality of results, time of simulation and memory allocation.

Given the aim of this study, the emphasis was attributed to the inner domain with a resolution of 1 km, which comprises the Douro Demarcated Region.

3.2. Study Period

The WRF-CHIMERE modelling system was applied to the DDR for the years 2003 to 2005, which were selected based on a climatological analysis of the years 1986 to 2005. Temperature was the most important meteorological factor when selecting those particular years, due to its clear association with ozone levels [44,45]. For each year of the period 1986–2005, the average temperature over the DDR from the 1st of April till the 30th of September was calculated by the WRF model with a resolution of 9 km (see Table 2).

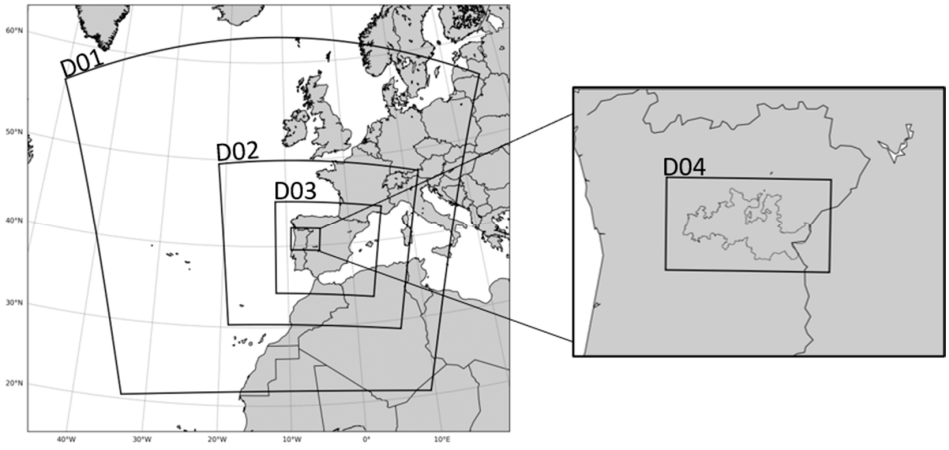

Figure 3. Simulated domains with the WRF-CHIMERE modelling system. (Spatial resolution: 81 km (D01), 27 km (D02), 9 km (D03) and 1 km (D04).

Table 2. Ranked Douro Demarcated Region (DDR) annual temperature (1 April–30 September) based on the Weather Research and Forecasting (WRF) model results (9 km resolution) forced by ERA-Interim for the period 1986–2005. Years in bold were selected for the simulations.

Rank	Year	Average Temperature (°C)
1	1987	17.92
2	1990	17.53
3	**2003**	**17.40**
4	1995	17.35
5	1989	17.25
6	**2005**	**17.23**
7	1997	17.16
8	1991	16.96
9	1999	16.85
10	**2004**	**16.71**
11	1998	16.69
12	1992	16.53
13	2001	16.38
14	1996	16.21
15	2000	16.14
16	2002	15.98
17	1993	15.85
18	1988	15.79
19	1986	15.76
20	1994	15.71
	Average 1986–2005	**16.67**

The three warmest consecutive years at DDR from the period 1986–2005 were 1989, 1990 and 1991. However, no observations were available at the Douro Norte monitoring station for this period. Considering the availability of O_3 measurements, the second three warmest consecutive years were selected for the simulations: 2003, 2004 and 2005 (from now

on referred to as recent past climate). The selected years showed larger temperature values than the averaged 1986–2005 along the vegetative period (see Table S1 in the supplementary material). This indicated a larger potential for ozone production, as desired for the ozone simulations.

3.3. Metrics of Assessment

The metrics to evaluate the effects of vegetation exposure to tropospheric ozone are related to the need of assessing the risk of phytotoxic damage with something quantifiable, that can be mapped, and thus contribute to the development of an emission control strategy.

There are several indicators to assess ozone exposure and the majority are based on ozone concentrations [11]. This paper will focus on a parameter established by the European legislation, the AOT40 accumulated exposure indicator. The AOT40 indicator, expressed in $\mu g \cdot m^{-3} \cdot h$, consisted of the sum of the difference between the values of hourly concentrations above 80 $\mu g \cdot m^{-3}$ and the value 80 $\mu g \cdot m^{-3}$, between 08:00 and 20:00 h of each day, between May and July (Equation (1)). Note that 80 $\mu g \cdot m^{-3}$ of ozone was approximately 40 ppb because the unit's conversion depends on the density of the air.

$$\text{AOT40} = \sum_{i=8h}^{20h} [[O_3] - 80]_i, \quad for\ [O_3] \geq\ 80\ \mu g \cdot m^{-3} \tag{1}$$

The AOT40 quantifies the ozone exposure, i.e., not the effective ozone uptake by vegetation. The target value established in the Air Quality Framework Directive 2008/50/EC is 18,000 $\mu g \cdot m^{-3} \cdot h$ averaged over 5 years. The long-term objective is 6000 $\mu g \cdot m^{-3} \cdot h$ and the advantage of the AOT40 approach is its simplicity because only ozone concentrations are required for its determination.

The assessment of the potential damage in terms of productivity and quality was done through the application of the exposure–response functions published by Soja et al. [21]. The functions were designed after a 4-year study of ozone uptake of pot-grown grapevines, fruit yield and sugar concentrations in juice, wherein 3 of the 4 years, grapevines were exposed to different ozone levels in open-top chambers. For this work, the third-year functions were applied to assess the scenario with the most damage for grapevines. Equation (2) shows the relationship between vineyard productivity and exposure to ozone, while Equation (3) relates to regards relative grape sugar production (AOT40 is expressed in $\mu mol \cdot mol^{-1} \cdot h$).

$$\text{productivity}\ (\%)\ = 102.4 - 2.614\ \text{AOT40} \tag{2}$$

$$\text{sugar}\ (\%) = 95.4 - 2.456\ \text{AOT40} \tag{3}$$

In addition to exposure levels, dry deposition levels were also calculated (Equation (4)). The results were based on the total O_3 dry deposition accumulated over May to July, the same period established for the calculation of the AOT40 indicator.

$$Dep\left(\text{g} \cdot \text{m}^{-2}\right) = \sum_{Mai}^{July} -v_d\ [O_3] \tag{4}$$

where,

Dep –dry deposition ($g \cdot m^{-2}$)
v_d —dry deposition velocity ($m \cdot s^{-1}$)
$[O_3]$ —ozone concentration ($g \cdot m^{-3}$)

CHIMERE models dry deposition of gases using the resistance scheme described by Wesely [46]. In this type of scheme, the dry deposition velocity is calculated using Equation (5).

$$v_d\left(m\ s^{-1}\right) = \frac{1}{r_a + r_b + r_c} \tag{5}$$

where,

v_d —dry deposition velocity ($m \cdot s^{-1}$)
r_a —aerodynamic resistance ($s \cdot m^{-1}$)
r_b —surface resistance ($s \cdot m^{-1}$)
r_c —canopy resistance ($s \cdot m^{-1}$)

The aerodynamic resistance (r_a) is related to the turbulent diffusion, the surface resistance (r_b) is dominated by molecular diffusion and the canopy resistance (r_c) is linked to the water solubility of the species. The latter was applied only to gaseous species and its formulation followed Erisman et al. [47] and the developments made in the EMEP model [12,48,49]. It is also related to other resistances such as the canopy stomatal resistance, soil resistance, mesophyll resistance, in-canopy aerodynamic resistance and external leaf resistance, which are dependent on the land use type and season. In general terms, it would be expected that the bulk canopy stomatal resistance represents approximately half of the total O_3 flux to the plant surface [50]. The bulk canopy non-stomatal resistance is also significant and can reach 20% or more of the total dry deposition [47]. The rest of the flux was conditioned by the R_a and R_b with R_b close to 1/3 of R_a. These ratios were also similar to those found by O_3 dry deposition modelling performed over a vineyard during the 1991 California Ozone Deposition Experiment [51].

In summary, dry deposition is considerably influenced by stomatal opening and the turbulent transport, which are influenced by wind speed, temperature, vapour pressure deficit, vegetation height, canopy closure and leaf index area (LAI).

3.4. Observation Data and Model Validation

Previously to the analysis of grapevines' exposure to ozone, the CHIMERE model performance was evaluated for the years 2003 to 2005 and for the period between April to September. For this, ozone model results were compared with observations. Within the domain D04, we have one air quality monitoring station only (Douro Norte). However, a model validation exercise considering one only observational dataset would not be robust enough for our analysis. We decided thus to include all the observational datasets located within a radius of 200 km of the DDR, using modelled data within D04, with 1 km resolution, whenever possible, or from D03, with 9 km resolution.

The selected stations included monitoring stations from the Portuguese and Spanish air quality monitoring networks, classified as background influence, that had more than 75% data collection efficiency during the simulation period and within a radius of 200 km of the DDR. Monitoring data were retrieved from the European air quality database (AirBase) [52]. Figure 4 shows the location of the selected air quality monitoring stations and the DDR.

The selected monitoring stations included six rural background stations, seven suburban and three urban stations, six of them belonging to the Spanish air quality monitoring network. Information on the location and characteristics of the stations is presented in Table 3.

The validation was based on the analysis of hourly time series plots and the standard statistical parameters [53], namely correlation coefficient (r), bias and root mean square error (RMSE) were calculated and are presented in Table 4.

In general, the statistical parameters showed that the CHIMERE model had an adequate performance for ozone simulations, with a correlation factor between 0.6 and 0.8, a mean bias of -12 $\mu g \cdot m^{-3}$, and an RMSE ranging between 18 and 37 $\mu g \cdot m^{-3}$. These results were similar or better than those obtained by other simulation studies with the CHIMERE model [54,55]. It should be noted that the BIAS was mostly positive, indicating that, overall, the model is overestimating the measured values. A systematic overestimation of surface ozone concentrations is reported in many CHIMERE studies. For example, at northwestern Iberian Peninsula and during the summer season, CHIMERE overestimated the ozone mean concentrations and underestimated the temporal variability of the daily maximum O_3 concentrations [56]. A specific study for Portugal [55] also reports overestimation of O_3

concentrations, with higher magnitude at suburban stations. However, when comparing CHIMERE with other air pollution models results over Europe [57], CHIMERE was found to have among the best skills for ozone daily maxima but to overestimated night-time ozone concentration, leading to a general positive bias not generally shared by other models [30]. In that intercomparison exercise, this bias is attributed in large part to overestimation of mixing in stable conditions.

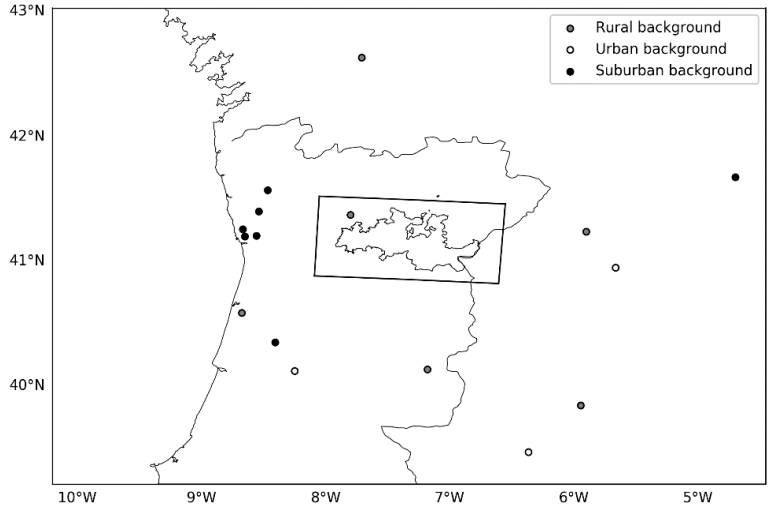

Figure 4. Location of the air quality monitoring stations considered for the model validation. The rectangular shape is the area of the D04 domain (1×1 km^2).

Table 3. List of stations used in model validation and its characteristics.

Code	Name	Type	Longitude (Degrees)	Latitude (Degrees)	Altitude (m)
DRN	Douro Norte	Rural	−7.79	41.37	1086
ERV	Ervedeira	Rural	−8.67	40.58	32
ES0013R	Peñausende	Rural	−5.89	41.23	985
ES0016R	O Saviñao	Rural	−7.70	42.63	506
ES1616A	Monfragüe	Rural	−5.93	39.84	376
FUN	Fundão	Rural	−7.17	40.13	473
CUS	Custóias-Matosinhos	Suburban	−8.64	41.20	100
ERM	Ermesinde-Valongo	Suburban	−8.55	41.20	140
ES1224A	Cementerio del Carmen	Suburban	−4.69	41.67	693
FRO	Frossos-Braga	Suburban	−8.46	41.57	51
ILH	Ílhavo	Suburban	−8.40	40.35	32
PER	Meco-Perafita	Suburban	−8.42	41.13	25
VNT	VN Telha-Maia	Suburban	−8.66	41.25	88
ES1449A	Salamanca	Urban	−5.65	40.94	797
ES1615A	Cáceres	Urban	−6.36	39.47	389
IGE	Instituto Geofísico de Coimbra	Urban	−8.24	40.12	147

Other possible reasons for overestimation of ozone concentrations include the use of an emissions inventory with low NO emissions. Close to the pollution sources (e.g., in urban and suburban areas) freshly emitted NO locally scavenges O_3, and thus missing NO emissions could lead to an overestimation of O_3 concentrations. This hypothesis could also explain an underestimation of O_3 concentrations in the areas downstream of the major precursor sources, as happens in Douro Norte (which is downstream important pollution sources in northwestern Portugal). The high values measured in this station have been widely discussed in several studies, and it is difficult to simulate its behavior [20,58].

When modelling ozone, it is important to simulate properly the maximum daily values. Time series of the maximum daily 8-h ozone mean levels between May and July (period for calculating AOT40 indicator) for the three simulated years are presented in

Figure 5. Note that Douro Norte station began measuring in 2004. Four "representative" sites were selected to cover the different type of monitoring stations.

Table 4. Correlation coefficient, bias, RMSE for each station, for O_3.

Code	Name	Type	r	Bias ($\mu g \cdot m^{-3}$)	RMSE ($\mu g \cdot m^{-3}$)
DRN	Douro Norte	Rural	0.7	−28.3	37.3
ERV	Ervedeira	Rural	0.7	2.9	23.3
ES0013R	Peñausende	Rural	0.7	−3.3	17.9
ES0016R	O Saviñao	Rural	0.6	12.0	21.5
ES1616A	Monfragüe	Rural	0.6	15.3	30.9
FUN	Fundão	Rural	0.7	13.3	26.4
CUS	Custóias-Matosinhos	Suburban	0.8	13.7	24.5
ERM	Ermesinde-Valongo	Suburban	0.8	13.6	24.8
ES1224A	Cementerio del Carmen	Suburban	0.8	17.5	29.2
FRO	Frossos-Braga	Suburban	0.6	28.2	36.9
ILH	Ílhavo	Suburban	0.6	19.3	31.9
PER	Meco-Perafita	Suburban	0.6	10.6	27.7
VNT	VN Telha-Maia	Suburban	0.7	14.3	26.2
ES1449A	Salamanca	Urban	0.7	20.4	30.1
ES1615A	Cáceres	Urban	0.6	11.9	30.7
IGE	Instituto Geofísico de Coimbra	Urban	0.7	26.0	34.6
	Average		**0.7**	**11.7**	**28.4**

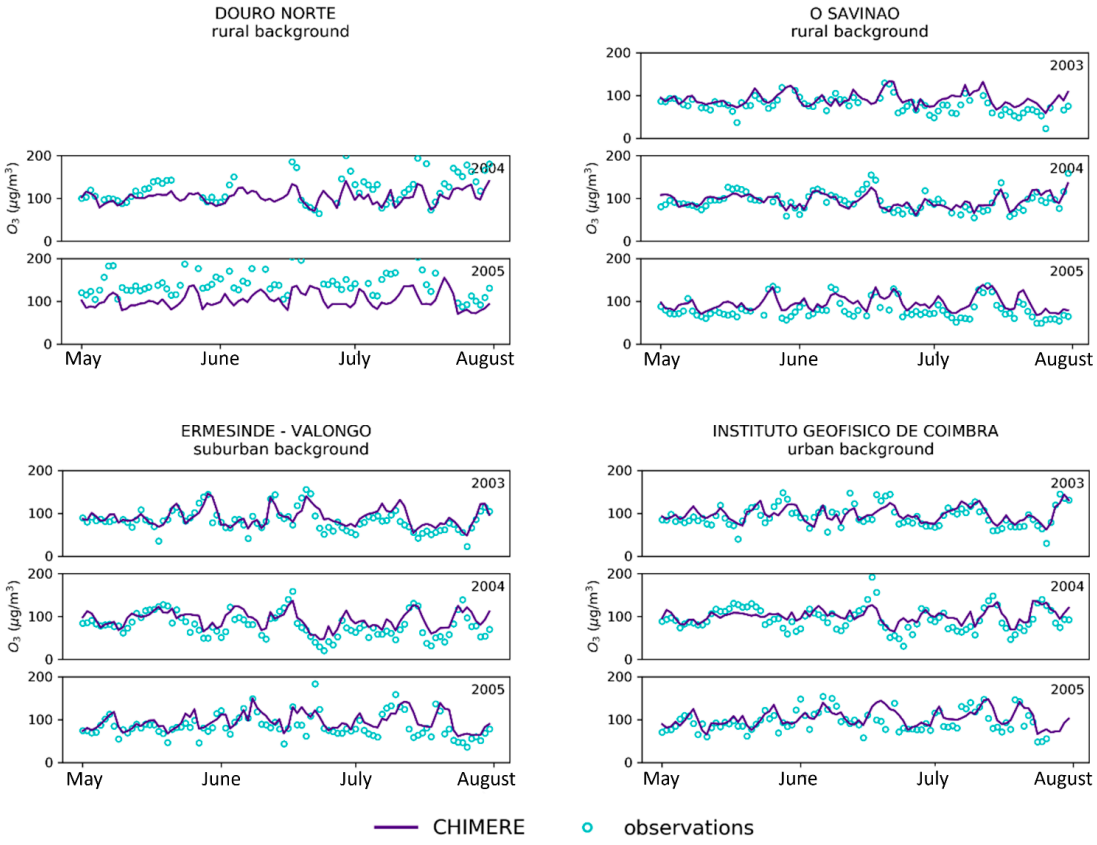

Figure 5. Observed and modelled maximum daily eight-hour mean ozone concentration for different types of monitoring stations.

In general, the model can simulate the daily maximum ozone variability. When concentrations are lower, the model tends to overestimate the O_3 levels, but, overall, it

reproduces the episodic events of high concentrations, with exception of the Douro Norte station, already mentioned before, which presents peculiar characteristics.

Although statistical performance indicators provide insight into the overall performance of the model, they do not indicate whether its performance has reached enough level of quality for a given application, e.g., policy decision support. The Delta Tool software (version 5.4) was used for additional tests. This tool was developed in the scope of the Forum on Air Quality Modelling in Europe [59,60] to assess quality criteria for the application of models under the Air Quality Framework Directive.

The Delta Tool uses mainly two indicators, the Model Quality Indicator (MQI) and the Model Quality Objective (MQO). The MQI is defined by the ratio between the BIAS and an amount proportional to the measurement uncertainty (Equation (6)).

$$\mathrm{MQI} = \frac{|O_i - M_i|}{2\,U_{95}(O_i)} \tag{6}$$

where,

O_i—observed value
M_i—simulated value
$U_{95}(O_i)$ —representative value of the measurement uncertainty, which corresponds to the 95th percentile highest value among all uncertainty values calculated (see [59] for additional details regarding the derivation of the observation uncertainty)

The MQO is defined as the minimum quality level to be achieved by the model to support the decision-making process; the objective is achieved when the MQI is less than or equal to 1.

One of the main features of this tool is called "target plot", which uses the MQI as the key indicator. The performance criteria for this indicator is defined by a circle boundary: if at least 90% of the stations are within the circle, the quality criteria are achieved. Figure 6 shows the target diagram obtained for the O_3 maximum daily 8-h mean for the summer period of 2004.

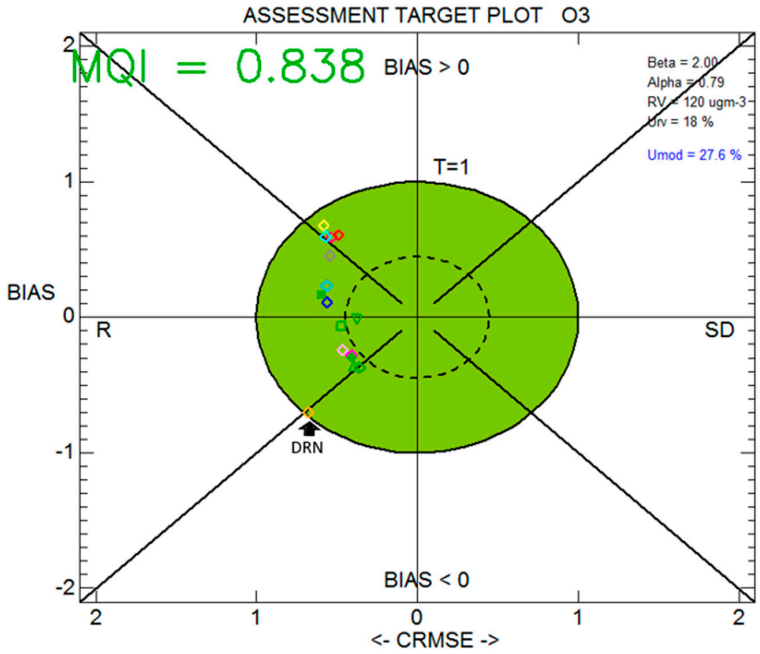

Figure 6. Target plot for the maximum daily 8-h mean values of ozone in the summer, obtained with the Delta Tool. The uncertainty parameters (Alpha, Beta, Reference Value (RV) and *U*rv) used to produce the diagram are listed on the top right-hand side together with the associated model uncertainty calculated by the DELTA software.

RV stands for Reference Value for a given time averaging usually based on reference values established by the Air Quality Directive. For ozone, RV = 120 $\mu g \cdot m^{-3}$. Urv represents the relative measurement uncertainty estimated around the reference value (RV) for a given time averaging. Alpha and Beta are other parameters related to the uncertainty formulation, which is detailed by [59].

The stations are all located on the left side, which means that the error associated with the correlation factor dominates in relation to the standard deviation. All stations are within the circle (MQI is less than 1) and the uncertainty associated with the model is less than 50% which meets the criteria established in the Air Quality Framework Directive.

Overall, and despite some limitations (such as the underestimation of ozone concentrations at the Douro Norte station with a bias of -28.3 $\mu g \cdot m^{-3}$, already discussed), the model validation exercise shows an adequate performance of the WRF-CHIMERE modelling system in simulating O_3 concentrations in the atmosphere, as shown by the fulfilment of the DELTA MQO. Thus, and always bearing in mind the uncertainty associated with the modelling methodology (27.6%), it is possible to state that the model results meet the necessary conditions to be used in this study.

4. Vineyard's Exposure to O_3

To assess the vineyard's exposure to O_3, the simulation results are shown as AOT40 (Equation (1)), calculated using the average of the 3 simulated years. Figure 7 presents the spatial distribution of AOT40 values for the Iberian Peninsula.

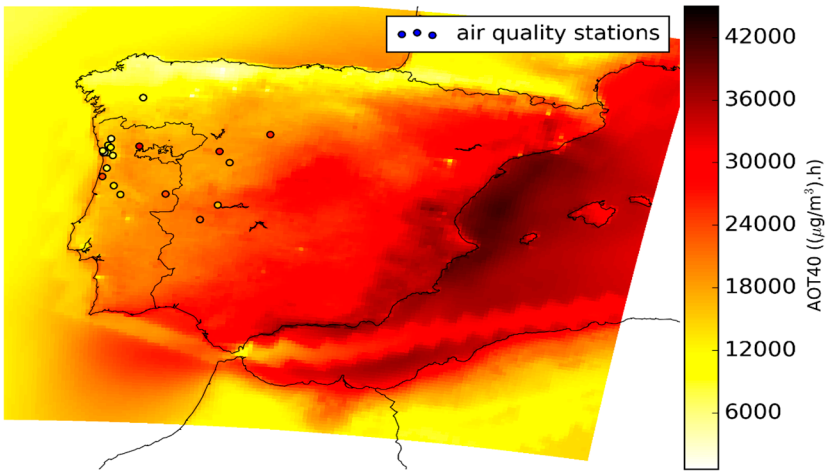

Figure 7. AOT40 levels ($\mu g \cdot m^{-3} \cdot h$) averaged for the 3 simulation years and over Iberian Peninsula (D03, 9 × 9 km^2 horizontal resolution). The circles represent the AOT40 levels measured by the air quality monitoring stations.

The higher levels of AOT40 were observed downstream of the major precursor sources (e.g., Madrid and Barcelona metropolitan areas) and along the eastern Iberian coast. Lower levels are observed in the North, indicating the effect of temperature in ozone formation (see Figure S1). Exceedances of the target value established by the Air Quality Framework Directive (18,000 $\mu g \cdot m^{-3} \cdot h$) were visible throughout the Iberian Peninsula, mainly in Spain.

The high values obtained in the Mediterranean Sea were probably related to the deposition processes of ozone, which are less efficient on water than on land (see Figure S2). Moreover, these concentrations may also be associated with the numerous ships that circulate the Mediterranean Sea, mainly in the summer period. When plumes containing nitrogen oxides react with the chloride in marine aerosols, high levels of nitrile chloride are produced. This compound is then photolyzed producing nitrogen dioxide that will accelerate the production of ozone. Gencarelli et al. [61] found that emissions from ships contributed approximately 20% to the levels of ozone in the Mediterranean Sea in 2003. Recent studies reinforce the role of shipping activities in the Mediterranean Sea as an

important source of O_3 precursors for the Mediterranean countries and the Mediterranean Basin itself [62–64]. In addition to local ozone production, transport mechanisms are also of great importance. The synoptic transport of pollution from Europe, that predominates in summer, is responsible for high concentrations of O_3 on the Mediterranean Sea (e.g., [65,66]). Duncan and Bey [67] show that the long-range transport of ozone generated from Europe contributed 5–20 ppb to countries bordering the Mediterranean Sea.

The circles in Figure 7 represent the AOT40 values calculated with the measured data. The target value for vegetation protection was exceeded in most rural stations, which means that pollutant's transport was causing high levels of ozone in areas where ozone production was not relevant. Furthermore, the model underestimated the AOT40 values measured in some rural background stations. These results are in agreement with the AOT40 maps, produced by the European Environment Agency [68], in terms of the range of values and spatial distribution.

Focusing on the area of interest, Figure 8 presents the AOT40 map for the DDR with a spatial resolution of 1 × 1 km^2.

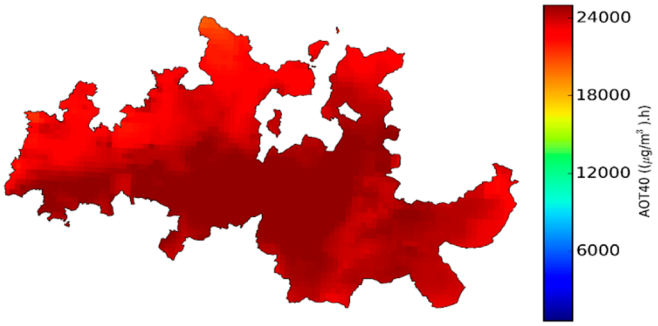

Figure 8. AOT40 levels (µg·m^{-3}·h) averaged for the 3 simulation years in the DDR (D04, 1 × 1 km^2 horizontal resolution).

Exceedances of the target value for vegetation protection were visible throughout the DDR, where the average AOT40 levels were approximately 22 500 µg.m^{-3}.h and the maximum levels could reach values of 24,000 µg·m^{-3}·h, about 1.3 times higher than the target value. The area where the effects of ozone exposure could be more damaging was in the Cima Corgo and Douro Superior sub-regions, which are the sub-regions with the lowest wine production per unit of area [69]. The high levels of estimated AOT40 in the region are worrying since they indicate that ozone concentrations may be causing direct damage to the grapevine and potentially diminishing its yield and quality. It is possible to quantify this damage by using exposure–response functions and the calculated AOT40 values. The functions from Soja et al. [21] were applied and Figures 9 and 10 show results for productivity and sugar content loss (expressed as a percentage), respectively.

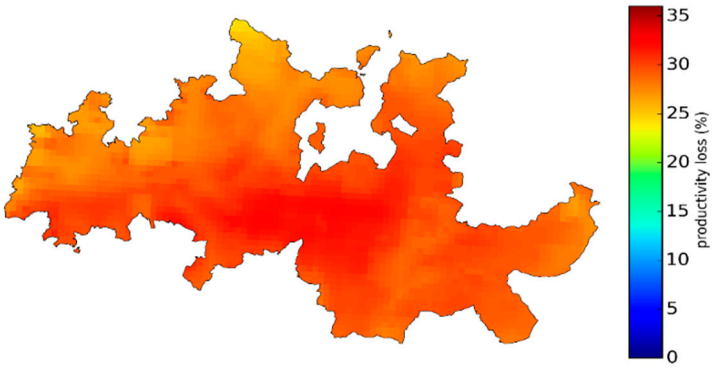

Figure 9. Productivity loss (%) in DDR (D04, 1 × 1 km^2 horizontal resolution), averaged for the 3 simulation years and based on Soja et al. (2004) exposure–response functions.

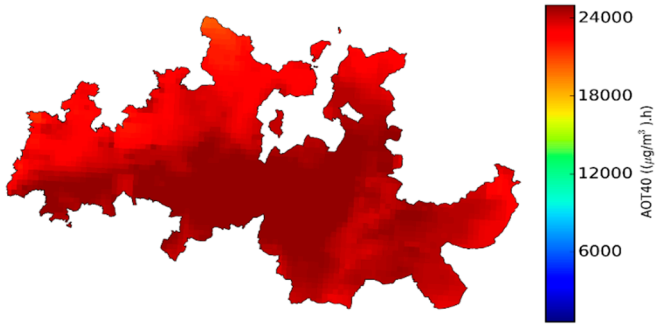

Figure 10. Sugar content loss (%) in DDR (D04, 1 × 1 km^2 horizontal resolution), averaged for the 3 simulation years and based on Soja et al. (2004) exposure–response functions.

The average productivity loss calculated for the simulation period in the DDR was 27% and the grapes' sugar loss was 32%. Being the sugar content a way of measuring the quality of wine, the estimated results could potentially represent a challenge for Douro's wine producers.

When discussing these outcomes, it is important to remember that although AOT40 is an important indicator for assessing the risk of vegetation exposure to ozone, it has some limitations. This indicator tends to overestimate vegetation damage since the concentration-damage ratio is not linear because it does not consider the uptake of ozone by the plants. Furthermore, applying Soja et al. [21] functions also brings uncertainty to the results, since the variety and age of the grapevines could also be related to greater or lesser plant tolerance to ambient ozone.

Although there is no defined threshold or dose–response functions for O_3 dry deposition for vineyards, considering the AOT40 limitations above mentioned the legislated indicator for vegetation protection should be based on the plants' ozone uptake instead of ozone exposure, as defended by Blanco-Ward et al. [11]. This potential new indicator could be based on O_3 dry deposition values. Therefore, averaged dry deposition values accumulated from May to July, the same AOT40 period, were calculated and their spatial distribution is presented in Figure 11.

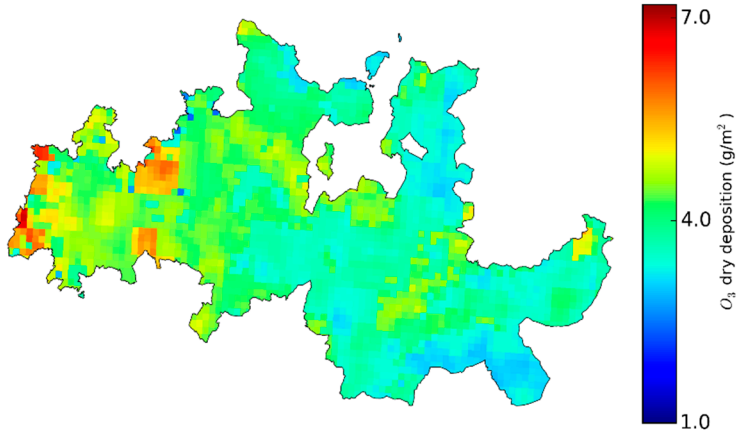

Figure 11. O_3 dry deposition (g·m^{-2}) in DDR (D04, 1 × 1 km^2 horizontal resolution), accumulated from May to July and averaged for the 3 simulation years.

The average accumulated dry deposition (May–July) for the DDR was approximately 4 g·m^{-2} (V_d ~ 0.64 cm/s) with a surface friction velocity of 3.5 m/s (R_a 26%, R_b 10%, R_c 65% with $R_{stomatal}$ 41% and $R_{nonstomatal}$ 24%). The highest values were observed in the Baixo Corgo sub-region (west side) and the lowest values in the Douro Superior sub-region (east side). This is likely because the Baixo Corgo sub-region is the area with more precipitation

and lower temperatures, which are more favorable conditions for stomatal opening and thus ozone uptake (see Table S1).

Comparing this spatial distribution with the AOT40 map (Figure 8), it is noticeable that the areas where the AOT40 values were higher did not correspond to the areas with higher values of dry deposition. This supports the conclusion that exposure-based indicators are not the best approach to assess ozone damage to vegetation. and that dose-based metrics are also needed to better support end-users.

5. Summary and Conclusions

The main objective of this study was to assess the Douro vineyards exposure to tropospheric ozone in past recent climate conditions. The air quality modelling system WRF-CHIMERE was applied to estimate O_3 concentrations and dry deposition levels and link them with the effects on sugar content and productivity of the grapevine. The simulations were performed and validated for the years 2003 to 2005, which were selected due to their hot summers, and the exposure indicator AOT40 was calculated as recommended by the Air Quality Framework Directive. The average calculated AOT40 value for the DDR was 22 500 $\mu g \cdot m^{-3} \cdot h$ suggesting that ozone concentrations in the DDR are very likely to bring damage to the vineyards.

Exposure–response functions from literature [21] were used to link the exposure of vineyards to productivity loss and sugar decrease. The estimated average productivity loss was 27% and the grapes' sugar loss was 32%. It is important to keep in mind the uncertainties of this approach and the obtained values. AOT40 is known for overestimating the damage to vegetation, besides, the established target value is for a generic crop that can have a different sensitivity to ozone than grapevines. Moreover, the exposure–response functions, though the best published option available at the time, also bring some uncertainty to the results as they are based on only one grapevine cultivar grown under continental climate conditions in an open-top-chamber.

Ozone dry deposition accumulated from May to July was approximately 4 $g \cdot m^{-2}$. Due to the lack of legislated values and bibliography, it is difficult to fully assess and discuss the obtained dry deposition values. Anyway, the areas where the AOT40 values were higher do not correspond to the ones of higher O_3 dry deposition. Hence, the risk of exposure to ozone based on the AOT40 could have been overestimated. In summary, to achieve more reliable results, future investigation would require the definition of a threshold for vegetation protection that considers the potential uptake by the vegetation using dry deposition levels, and to continue to develop grapevine-specific dose–response functions.

Finally, climate change scenario projections point to an increase in ozone concentrations [70], which means that the effects of ozone on the grapevine may be aggravated, while some studies indicate that climate changes will benefit wine production [71,72]. Therefore, as future work, we will assess this dynamic by performing ozone simulations in the DDR for future climate and calculating bioclimatic indicators to assess the vineyard quality and performance.

Supplementary Materials: The following are available online at https://www.mdpi.com/2073-4433/12/2/200/s1, Figure S1: Temperature (°C) averaged between May and July over Iberian Peninsula (D03, 9 x 9 km^2 horizontal resolution), Figure S2: O_3 dry deposition ($g.cm^{-2}$) on Iberian Peninsula (D03, 9 x 9 km^2 horizontal resolution), accumulated from May to July and averaged for the 3 simulation year, Table S1: Average precipitation (mm) and temperature (°C) for Baixo Corgo and Douro Superior sub-regions between May and July for 2003 to 2005.

Author Contributions: conceptualization, A.A., A.M., C.B., M.L. and A.I.M.; formal analysis, A.A. and C.V.; investigation, A.A.; project administration, C.S. and A.I.M.; software, A.A., C.G., D.B.-W., C.V. and V.R.; supervision, A.R. and A.I.M.; visualization, C.G.; writing—original draft, A.A.; writing—review and editing, A.A., C.G., D.B.-W., A.M., C.S., C.V., V.R., A.R., C.B., M.L. and A.I.M. All authors have read and agreed to the published version of the manuscript.

Funding: The authors wish to thank the financial support of FEDER through the COMPETE Programme and the national funds from FCT—Science and Technology Portuguese Foundation for financing the DOUROZONE project (PTDC/AAG-MAA/3335/2014; POCI-01-0145-FEDER-016778). Thanks are also due for the financial support to the PhD grants of A. Ascenso (SFRH/BD/136875/2018) and C. Silveira (SFRH/BD/112343/2015), Thanks are due to FCT/MCTES for the financial support to CESAM (UIDP/50017/2020+UIDB/50017/2020), through national funds.

Institutional Review Board Statement: Not applicable.

Informed Consent Statement: Not applicable.

Conflicts of Interest: The authors declare no conflict of interest.

References

1. Environmental Protection Agency (EPA). Air quality criteria for ozone and related photochemical oxidants volume I of III. *Environ. Prot.* **2006**, *1*, 820.
2. Feng, Z.; Kobayashi, K.; Ainsworth, E.A. Impact of elevated ozone concentration on growth, physiology, and yield of wheat (Triticum aestivum L.): A meta-analysis. *Glob. Chang. Biol.* **2008**, *14*, 2696–2708. [CrossRef]
3. Simpson, D.; Ashmore, M.R.; Emberson, L.; Tuovinen, J.-P. A comparison of two different approaches for mapping potential ozone damage to vegetation. A model study. *Environ. Pollut.* **2007**, *146*, 715–725. [CrossRef]
4. Ainsworth, E.; Yendrek, C.R.; Sitch, S.; Collins, W.J.; Emberson, L.D. The effects of tropospheric ozone on net primary productivity and implications for climate change. *Annu. Rev. Plant Biol.* **2012**, *63*, 637–661. [CrossRef]
5. Black, V.J.; Black, C.R.; Roberts, J.A.; Stewart, C.A. Impact of ozone on the reproductive development of plants. *New Phytol.* **2000**, *147*, 421–447. [CrossRef]
6. Heck, W.W.; Taylor, O.C.; Adams, R.; Bingham, G.; Miller, J.; Preston, E.; Weinstein, L. Assessment of crop loss from ozone. *J. Air Pollut. Control. Assoc.* **1982**, *32*, 353–361. [CrossRef]
7. Holland, M.; Kinghorn, S.; Emberson, L.; Cinderby, S.; Ashmore, M.; Mills, G.; Harmens, H. Development of a framework for probabilistic assessment of the economic losses caused by ozone damage to crops in Europe. *Nat. Environ. Res. Counc. CEH* **2006**, *1*, 3–205.
8. Karlsson, P.E.; Pleijel, H.; Belhaj, M.; Danielsson, H.; Dahlin, B.; Andersson, M.; Hansson, M.; Munthe, J.; Grennfelt, P. Economic assessment of the negative impacts of ozone on crop yields and forest production. A case study of the estate Ostads Säteri in southwestern Sweden. *AMBIO* **2005**, *34*, 32–40. [CrossRef] [PubMed]
9. Mills, G.; Hayes, F.; Simpson, D.; Emberson, L.; Norris, D.; Harmens, H.; Büker, P. Evidence of widespread effects of ozone on crops and (semi-)natural vegetation in Europe (1990–2006) in relation to AOT40- and flux-based risk maps. *Glob. Chang. Biol.* **2010**, *17*, 592–613. [CrossRef]
10. Avnery, S.; Mauzerall, D.L.; Liu, J.; Horowitz, L.W. Global crop yield reductions due to surface ozone exposure: 2. Year 2030 potential crop production losses and economic damage under two scenarios of O3 pollution. *Atmos. Environ.* **2011**, *45*, 2297–2309. [CrossRef]
11. Blanco-Ward, D.; Ribeiro, A.; Paoletti, E.; Miranda, A.I. Assessment of tropospheric ozone phytotoxic effects on the grapevine (Vitis vinifera L.): A review. *Atmos. Environ.* **2021**, *244*, 117924. [CrossRef]
12. Emberson, L.D.; Ashmore, M.R.; Cambridge, H.M.; Simpson, D.G.; Tuovinen, J.P. Modelling stomatal ozone flux across Europe. *Environ. Pollut.* **2000**, *109*, 403–413. [CrossRef]
13. Mauzerall, D.L.; Wang, X. Protectingagriculturalcrops from theeffects oftroposphericozoneexposure: Reconciling Science and Standard Setting in the United States, Europe, and Asia. *Annu. Rev. Energy Environ.* **2001**, *26*, 237–268. [CrossRef]
14. Pellegrini, E.; Campanella, A.; Paolocci, M.; Trivellini, A.; Gennai, C.; Muganu, M.; Nali, C.; Lorenzini, G. Functional leaf traits and diurnal dynamics of photosynthetic parameters predict the behavior of grapevine varieties towards ozone. *PLoS ONE* **2015**, *10*, e0135056. [CrossRef]
15. Emberson, L.D.; Simpson, D.; Ashmore, M.R.; Cambridge, H.M. *Towards a Model of Ozone Deposition and Stomatal Uptake over Europe*; The Norwegian Meteorological Institute: Oslo, Norway, 2000.
16. Pleijel, H.; Danielsson, H.; Emberson, L.; Ashmore, M.R.; Mills, G. Ozone risk assessment for agricultural crops in Europe: Further development of stomatal flux and flux–response relationships for European wheat and potato. *Atmos. Environ.* **2007**, *41*, 3022–3040. [CrossRef]
17. Castagna, A.; Ranieri, A. Detoxification and repair process of ozone injury: From O3 uptake to gene expression adjustment. *Environ. Pollut.* **2009**, *157*, 1461–1469. [CrossRef]
18. Musselman, R.C.; Lefohn, A.S.; Massman, W.J.; Heath, R.L. A critical review and analysis of the use of exposure- and flux-based ozone indices for predicting vegetation effects. *Atmos. Environ.* **2006**, *40*, 1869–1888. [CrossRef]
19. Grünhage, L.; Krupa, S.; Legge, A.; Jäger, H.-J. Ambient flux-based critical values of ozone for protecting vegetation: Differing spatial scales and uncertainties in risk assessment. *Atmos. Environ.* **2004**, *38*, 2433–2437. [CrossRef]
20. Monteiro, A.; Strunk, A.; Carvalho, A.; Tchepel, O.; Miranda, A.I.; Borrego, C.; Saavedra, S.; Rodriguez, A.; Souto, J.; Casares, J.; et al. Investigating a high ozone episode in a rural mountain site. *Environ. Pollut.* **2012**, *162*, 176–189. [CrossRef]

21. Soja, G.; Reichenauer, T.G.; Eid, M.; Soja, A.-M.; Schaber, R.; Gangl, H. Long-term ozone exposure and ozone uptake of grapevines in open-top chambers. *Atmos. Environ.* **2004**, *38*, 2313–2321. [CrossRef]
22. Jones, G. *Uma Avaliação Do Clima Para a Região Demarcada Do Douro: Uma Análise das Condições Climáticas Do Passado, Presente e Futuro Para a Produção de Vinho*; ADVID—Associação para o Desenvolvmento da Viticultura Duriense: Peso da Régua, Portugal, 2013; Available online: http://www.advid.pt/imagens/noticias/livro_PT_FinalWEB.pdf. (accessed on 1 January 2021)(In Prortugese). ISBN 9789899836808.
23. Bateira, C.; Martins, L.; Santos, M.; Pereira, S. *Cartografia da Susceptibilidade a Movimentos de Vertente na Região Demarcada do Douro*; Universidade Lusófona: Porto, Portugal, 2011. (In portuguese)
24. Santos, J.A.; Fraga, H.; Malheiro, A.C.; Moutinho-Pereira, J.; Dinis, L.T.; Correia, C.; Moriondo, M.; Leolini, L.; Dibari, C.; Costafreda-Aumedes, S.; et al. A review of the potential climate change impacts and adaptation options for European viticulture. *Appl. Sci.* **2020**, *9*, 3092. [CrossRef]
25. Cogato, A.; Meggio, F.; Pirotti, F.; Cristante, A.; Marinello, F. Analysis and impact of recent climate trends on grape composition in north-east Italy. *BIO Web Conf.* **2019**, *13*, 04014. [CrossRef]
26. Miranda, A.I.; Rocha, A.; Ribeiro, A.; Monteiro, A. (Eds.) *Dourozone—Risco de Exposição ao Ozono Para a Vinha Duriense em Clima Atual e Futuro*; UA Editora—Universidade de Aveiro: Aveiro, Portugal, 2018; ISBN 9789727895526. (In Portuguese)
27. General Directorate for Territorial Development. A land cover/use map of mainland Portugal for 2010. *Sustainability* **2017**, *9*, 351.
28. Carvalho, A.; Monteiro, A.; Ribeiro, I.; Tchepel, O.; Miranda, A.I.; Borrego, C.; Saavedra, S.; Souto, J.A.; Casares, J.J. High ozone levels in the northeast of Portugal: Analysis and characterization. *Atmos. Environ.* **2010**, *44*, 1020–1031. [CrossRef]
29. Borrego, C.; Monteiro, A.; Martins, H.; Ferreira, J.; Fernandes, A.P.; Rafael, S.; Miranda, A.I.; Guevara, M.; Baldasano, J.M. Air quality plan for ozone: An urgent need for North Portugal. *Air Qual. Atmos Health* **2015**, *9*, 447–460. [CrossRef]
30. Menut, L.; Bessagnet, B.; Khvorostyanov, D.; Beekmann, M.; Blond, N.; Colette, A.; Coll, I.; Curci, G.; Foret, G.; Hodzic, A.; et al. Chimere 2013: A model for regional atmospheric composition modelling. *Geosci. Model Dev.* **2013**, *6*, 981–1028. [CrossRef]
31. Mailler, S.; Menut, L.; Khvorostyanov, D.; Valari, M.; Couvidat, F.; Siour, G.; Turquety, S.; Briant, R.; Tuccella, P.; Bessagnet, B.; et al. Chimere-2017: From urban to hemispheric chemistry-transport modeling. *Geosci. Model Dev.* **2017**, *10*, 2397–2423. [CrossRef]
32. Skamarock, C.; Klemp, B.; Dudhia, J.; Gill, O.; Barker, D.; Duda, G.; Huang, X.; Wang, W.; Powers, G. *A Description of the Advanced Research WRF Version 3*; Technical Report for University Corporation for Atmospheric Research: Boulder, CO, USA, 2008.
33. Dee, D.P.; Uppala, S.M.; Simmons, A.J.; Berrisford, P.; Poli, P.; Kobayashi, S.; Andrae, U.; Balmaseda, M.A.; Balsamo, G.; Bauer, P.; et al. The ERA-Interim reanalysis: Configuration and performance of the data assimilation system. *Q. J. R. Meteorol. Soc.* **2011**, *137*, 553–597. [CrossRef]
34. Marta-Almeida, M.; Teixeira, J.C.; Carvalho, M.J.; Melo-Gonçalves, P.; Rocha, A.M. High resolution WRF climatic simulations for the Iberian Peninsula: Model validation. *Phys. Chem. Earth Parts A B C* **2016**, *94*, 94–105. [CrossRef]
35. Schmidt, H. A comparison of simulated and observed ozone mixing ratios for the summer of 1998 in Western Europe. *Atmos Environ.* **2001**, *35*, 6277–6297. [CrossRef]
36. Bessagnet, B.; Hodzic, A.; Vautard, R.; Beekmann, M.; Cheinet, S.; Honoré, C.; Liousse, C.; Rouil, L. Aerosol modeling with CHIMERE—preliminary evaluation at the continental scale. *Atmos. Environ.* **2004**, *38*, 2803–2817. [CrossRef]
37. Vautard, R.; Honore, C.; Beekmann, M.; Rouil, L. Simulation of ozone during the august 2003 heat wave and emission control scenarios. *Atmos. Environ.* **2005**, *39*, 2957–2967. [CrossRef]
38. Hauglustaine, D.A.; Hourdin, F.; Jourdain, L.; Filiberti, M.-A.; Walters, S.; Lamarque, J.-F.; Holland, E.A. Interactive chemistry in the Laboratoire de Météorologie Dynamique general circulation model: Description and background tropospheric chemistry evaluation. *J. Geophys. Res. Space Phys.* **2004**, *109*. [CrossRef]
39. Ginoux, P.; Chin, M.; Tegen, I.; Prospero, J.M.; Holben, B.; Dubovik, O.; Lin, S.-J. Sources and distributions of dust aerosols simulated with the GOCART model. *J. Geophys. Res. Space Phys.* **2001**, *106*, 20255–20273. [CrossRef]
40. Vestreng, V.; Adams, M.; Goodwin, J. *Inventory Review 2004—Emission Data Reported to CLRTAP and under the NEC Directive*; EMEP/EEA Joint Review Report; Meteorological Synthesizing Centre-West of EMEP; The Norwegian Meteorological Institute: Oslo, Norway, 2004; ISSN 0804-2446.
41. Guenther, A.; Karl, T.; Harley, P.; Wiedinmyer, C.; Palmer, P.I.; Geron, C. Estimates of global terrestrial isoprene emissions using MEGAN (Model of Emissions of Gases and Aerosols from Nature). *Atmos. Chem. Phys.* **2006**, *6*, 3181–3210. [CrossRef]
42. Derognat, C.; Baeumle, M.; Beekmann, M.; Martin, D.; Schmidt, H. Effect of biogenic volatile organic compound emissions on tropospheric chemistry during the atmospheric pollution over the Paris Area (ESQUIF) campaign in the Ile-de-France region. *J. Geophys. Res. Space Phys. Atmos.* **2003**, *108*. [CrossRef]
43. Carter, W.P.L. A detailed mechanism for the gas-phase atmospheric reactions of organic compounds. *Atmos. Environ. Part A Gen. Top.* **1990**, *24*, 481–518. [CrossRef]
44. Gu, Y.; Li, K.; Xu, J.; Liao, H.; Zhou, G. Observed dependence of surface ozone on increasing temperature in Shanghai, China. *Atmos. Environ.* **2020**, *221*, 117108. [CrossRef]
45. Porter, W.C.; Heald, C.L. The mechanisms and meteorological drivers of the summertime ozone–temperature relationship. *Atmos. Chem. Phys. Discuss.* **2019**, *19*, 13367–13381. [CrossRef]
46. Wesely, M.L. Parameterization of surface resistances to gaseous dry deposition in regional-scale numerical models. *Atmos. Environ.* **1989**, *23*, 1293–1304. [CrossRef]

47. Erisman, J.W.; Van Pul, A.; Wyers, P. Parametrization of surface resistance for the quantification of atmospheric deposition of acidifying pollutants and ozone. *Atmos. Environ.* **1994**, *28*, 2595–2607. [CrossRef]
48. Simpson, D.; Benedictow, A.; Berge, H.; Bergstrom, R.; Emberson, L.D.; Fagerli, H.; Flechard, C.R.; Hayman, G.D.; Gauss, M.; Jonson, J.E.; et al. The EMEP MSC-W chemical transport model—Technical description. *Atmos. Chem. Phys.* **2012**, *12*, 7825–7865. [CrossRef]
49. Simpson, D.; Tuovinen, J.-P.; Emberson, L.; Ashmore, M.R. Characteristics of an ozone deposition module II: Sensitivity analysis. *Water Air Soil Pollut.* **2003**, *143*, 123–137. [CrossRef]
50. Franz, M.; Simpson, D.; Arneth, A.; Zaehle, S. Development and evaluation of an ozone deposition scheme for coupling to a terrestrial biosphere model. *Biogeosciences* **2017**, *14*, 45–71. [CrossRef]
51. Padro, J.; Massman, W.J.; Den Hartog, G.; Neumann, H.H. Dry deposition velocity of O3 over a vineyard obtained from models and observations: The 1991 California ozone deposition experiment. *Water Air Soil Pollut.* **1994**, *75*, 307–323. [CrossRef]
52. European Environment Agency (EEA). AirBase—The European Air Quality Database. Available online: https://www.eea.europa.eu/data-and-maps/data/airbase-the-european-air-quality-database-8#tab-figures-produced (accessed on 5 December 2016).
53. Borrego, C.; Monteiro, A.; Ferreira, J.; Miranda, A.I.; Costa, A.M.; Carvalho, A.C.; Lopes, M. Procedures for estimation of modelling uncertainty in air quality assessment. *Environ. Int.* **2008**, *34*, 613–620. [CrossRef]
54. Falasca, S.; Curci, G. High-resolution air quality modeling: Sensitivity tests to horizontal resolution and urban canopy with WRF-CHIMERE. *Atmos. Environ.* **2018**, *187*, 241–254. [CrossRef]
55. Russo, M.A.; Gama, C.; Monteiro, A. How does upgrading an emissions inventory affect air quality simulations? *Air Qual. Atmos Healh* **2019**, *12*, 731–741. [CrossRef]
56. Brands, S.; Fernández-García, G.; Vivanco, M.; Tesouro Montecelo, M.; Gallego Fernández, N.; David Saunders Estévez, A.; Enrique Carracedo García, P.; Neto Venâncio, A.; Melo Da Costa, P.; Costa Tomé, P.; et al. An exploratory performance assessment of the CHIMERE model (version 2017r4) for the northwestern Iberian Peninsula and the summer season. *Geosci. Model Dev.* **2020**, *13*, 3947–3973. [CrossRef]
57. Vautard, R.; Schaap, M.; Bergström, R.; Bessagnet, B.; Brandt, J.; Builtjes, P.J.H.; Christensen, J.H.; Cuvelier, C.; Foltescu, V.; Graff, A.; et al. Skill and uncertainty of a regional air quality model ensemble. *Atmos. Environ.* **2009**, *43*, 4822–4832. [CrossRef]
58. Monteiro, A.; Gouveia, S.; Scotto, M.G.; Lopes, J.; Gama, C.; Feliciano, M.; Miranda, A.I. Investigating ozone episodes in Portugal: A wavelet-based approach. *Air Qual. Atmos Health* **2015**, *9*, 775–783. [CrossRef]
59. Thunis, P.; Pernigotti, D.; Gerboles, M. Model quality objectives based on measurement uncertainty. Part I: Ozone. *Atmos. Environ.* **2013**, *79*, 861–868. [CrossRef]
60. Thunis, P.; Pederzoli, A.; Pernigotti, D. Performance criteria to evaluate air quality modeling applications. *Atmos. Environ.* **2012**, *59*, 476–482. [CrossRef]
61. Gencarelli, C.N.; Hedgecock, I.M.; Sprovieri, F.; Schürmann, G.J.; Pirrone, N. Importance of ship emissions to local summertime ozone production in the mediterranean marine boundary layer: A Modeling study. *Atmosphere* **2014**, *5*, 937–958. [CrossRef]
62. Pay, M.-T.; Gangoiti, G.; Guevara, M.; Napelenok, S.; Querol, X.; Jorba, O.; García-Pando, C.P. Ozone source apportionment during peak summer events over southwestern Europe. *Atmos. Chem. Phys.* **2019**, *19*, 5467–5494. [CrossRef]
63. Lupascu, A.; Butler, T. Source attribution of European surface O3 using a tagged O3 mechanism. *Atmos. Chem. Phys.* **2019**, *19*, 14535–14558. [CrossRef]
64. Tagaris, E.; Stergiou, I.; Sotiropoulou, R.P. Impact of shipping emissions on ozone levels over Europe: Assessing the relative importance of the Standard Nomenclature for Air Pollution (SNAP) categories. *Environ. Sci. Pollut. Res.* **2017**, *24*, 14903–14909. [CrossRef]
65. Duncan, B.N.; West, J.J.; Yoshida, Y.; Fiore, A.M.; Ziemke, J.R. The influence of European pollution on ozone in the Near East and northern Africa. *Atmos. Chem. Phys. Discuss.* **2008**, *8*, 2267–2283. [CrossRef]
66. Kallos, G.; Kotroni, V.; Lagouvardos, K.; Papadopoulos, A. On the Long-Range transport of air pollutants from Europe to Africa. *Geophys. Res. Lett.* **1998**, *25*, 619–622. [CrossRef]
67. Duncan, B.N.; Bey, I. A modeling study of the export pathways of pollution from Europe: Seasonal and interannual variations (1987–1997). *J. Geophys. Res. Space Phys.* **2004**, *109*. [CrossRef]
68. European Environment Agency (EEA) Ozone AOT40 for Crops. 2004. Available online: https://www.eea.europa.eu/data-and-maps/figures/ozone-aot40-for-crops-2004 (accessed on 18 December 2020).
69. Insituto DOS Vihnos do Douro e Porto. IVDP—Estatística Geral. Available online: www.ivdp.pt (accessed on 12 December 2018).
70. Carvalho, A.; Monteiro, A.; Solman, S.; Miranda, A.I.; Borrego, C. Climate-driven changes in air quality over Europe by the end of the 21st century, with special reference to Portugal. *Environ. Sci. Policy* **2010**, *13*, 445–458. [CrossRef]
71. Sacchelli, S.; Fabbrizzi, S.; Menghini, S. Climate change effects and adaptation strategies in the wine sector: A quantitative literature review. *Wine Econ. Policy* **2016**, *5*, 114–126. [CrossRef]
72. Brainard, J.S.; Jones, A.P.; Bateman, I.J.; Lovett, A.; Fallon, P.J. Modelling Environmental equity: Access to air quality in birmingham, england. *Environ. Plan. A Econ. Space* **2002**, *34*, 695–716. [CrossRef]